Novel Effects of Metal Ion Chelation on the Properties of Lipoic Acid-Capped Ag and Au Nanoparticles

Sheela Berchmans, P. John Thomas, and C. N. R. Rao*

Chemistry and Physics of Materials Unit, Jawaharlal Nehru Centre for Advanced Scientific Research, Jakkur, Bangalore 560 064, India

Received: October 23, 2001; In Final Form: January 31, 2002

The effects of the interactions of metal ions with lipoic acid-capped Ag and Au nanoparticles have been studied by the combined use of electronic absorption spectroscopy and transmission electron microscopy. Three types of effects that are dependent on the metal ion concentration can be distinguished. First, in the dilute regime, there is reversible chelation of the metal ions, causing a marked dampening of the plasmon resonance band of the nanoparticles, but there is no aggregation. The magnitude of plasmon dampening depends on the nature as well as the concentration of the metal ions. In the intermediate concentration regime, aggregation occurs, but in the high concentration regime, there is precipitation. These different regimes are clearly evidenced in the changes in the electronic spectra and in the electron micrographs.

Introduction

Nanoparticles of gold and silver have characteristic absorption bands in the electronic spectra because of plasmon resonance.[1,2] The plasmon absorption bands are found even when the nanoparticles are covered with various capping agents and have been utilized to probe the growth and agglomeration of the nanoparticles and chemisorption at their surfaces.[3−5] The dampening of the plasmon band of nanoparticles following the chemisorption of thiols has been examined by Linnert et al.[5] Flocculation rates of Au nanocrystals stabilized by thiols of the form $HS(CH_2)_nR$ (R = alkyl or carbonyl group) have been studied in terms of the flocculation parameter, which is the intergrated area between 600 and 800 nm in the absorption spectra.[6] The flocculation rates are pH-dependent.[7] When a mercaptocarboxylic acid is used as the capping agent, the thiol end binds to the metal nanoparticle with the carboxyl end sticking out radially, enabling chelation by metal ions.[8−11] Templeton et al.[9] have obtained a layer-by-layer assembly of Au nanocrystals on an Au surface, making use of the ability of the metal ion to coordinate between two layers of the nanocrystals. It has been suggested that the colorimetric response of such Au nanocrystals could be useful in sensing heavy metals that chelate with the carboxyl group.[10] Furthermore, pH titrations carried out by Simard et al.[11] reveal the reversible nature of the aggregates produced by chelation.

We have carried out a systematic investigation of the interaction of metal ions with α-lipoic acid (thioctic acid or 1,2-dithiolane-3-pentanoic acid) -capped Ag and Au nanoparticles by means of electronic absorption spectroscopy and transmission electron microscopy. In this paper, we report different types of changes that take place in metal colloids when the carboxyl functional group attached to the tail of the amphipilic capping agent interacts with metal ions. We show two possible ways metal ions can bind to the carboxyl end of lipoic acid in Figure 1. We observe three types of changes depending on the concentration of the metal ions used. The observed changes are specific to the metal ions and are useful in helping one to distinguish different metal ions present in a solution.

Experimental Section

Metal nanoparticles capped by α-lipoic acid were prepared by a slight modification of the procedure reported by Maya et al.[12] The procedure involves the addition of 15 mL of 2.5 mM $NaBH_4$ to a 15-mL aqueous solution containing 75 μmols each of $HAuCl_4$ and α-lipoic acid to obtain a wine-red sol containing nanoparticles of gold. The sol was thoroughly aerated with argon and repeatedly extracted with dicholromethane to remove unreacted products. Nanoparticles of Ag capped with α-lipoic acid could be obtained by starting with $AgNO_3$. The sols thus obtained were examined with a JEOL-3010 transmission electron microscope (TEM) operating at 300 kV and were further characterized by UV−visible spectroscopy carried out with a Perkin-Elmer lambda 900 spectrometer. Samples for TEM were prepared by depositing a drop of the sol on a holey carbon grid and allowing it to dry in air and then in a desiccator overnight. The mean diameter and the size distribution were determined from the TEM images and represent averages over a few hundred nanoparticles. The mean diameter of the nanocrystals could be varied by changing the starting metal/lipoic acid ratios. Thus, Au/lipoic acid molar ratios of 1:1 and 1:2.5 yielded particles of diameter 7.5 ± 0.7 nm and 3.0 ± 0.4 nm, respectively, and Ag/lipoic acid ratios of 1:2 and 1:5 yielded particles of diameter 5 ± 0.4 nm and 2.6 ± 0.4 nm, respectively.

Stock solutions of 1 mM $CuSO_4$, $FeSO_4$ (pH ≈ 3), $Ni(NO_3)_2$ and acetates of Mn, Cd, Zn, and Pb were used as sources of the metal ions, whose interactions with the lipoic acid-capped metal nanoparticles were studied. Stock solutions of higher concentrations were used when necessary. A few microliters of the stock solution were directly added to the sols in quartz cuvettes to follow the changes accompanying the increase in concentration of the metal ions. We have given metal-ion concentrations in units of μM. Aliquots of the sol containing metal ions were drawn at periodic intervals to carry out TEM measurements. The sols containing the metal ions remained stable and optically clear over periods of several weeks. The above experiments were

* Corresponding author. E-mail: cnrrao@jncasr.ac.in.
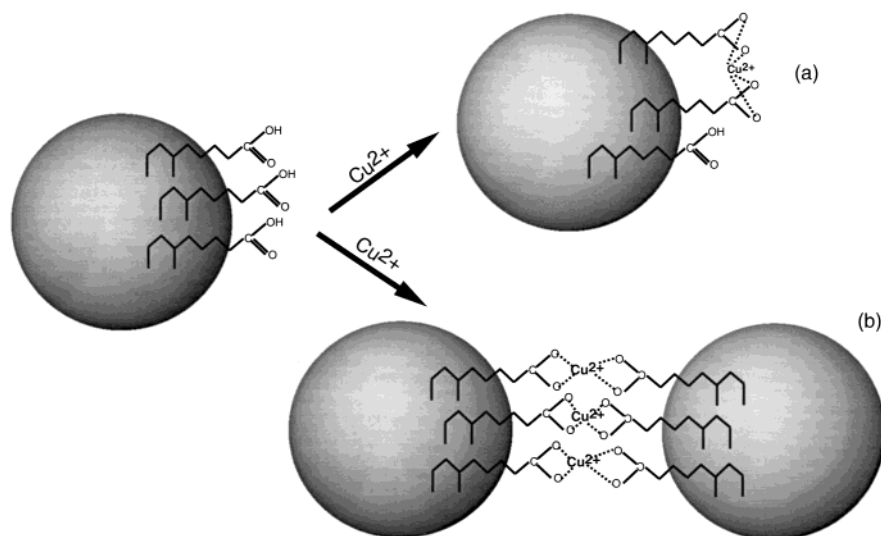
Figure 1. Schematic illustration showing the binding of metal ions to the carboxyl groups present at the tail of the amphiphile capping the metal nanoparticles. In (a), the metal ion is bound to the carboxyl end of one nanoparticle, but in (b), it binds to the carboxyls of two nanoparticles.

also carried out in the presence of poly(vinyl alcohol) (PVA, 5%). Quantitatively similar results were obtained with PVA except in the high concentration regime, as detailed in the Results and Discussion section.

Infrared spectra of the lipoic acid-covered nanoparticles before and after chelation (with excess Cu ions) showed the change from the carboxyl group to the carboxylate anion.

Results and Discussion

Figure 2 shows the changes in the absorption spectra of Ag nanoparticles of ∼5-nm diameter capped by α-lipoic acid following the addition of Cu^{2+} and Fe^{2+} ions. In the absence of metal ions, the plasmon band is observed at ∼430 nm. As Cu^{2+} or Fe^{2+} ions are added in the form of aqueous solutions, the plasmon band is dampened in proportion to the concentration of the metal ion (see Figure 2). After the addition of the metal ion, the plasmon-band intensity immediately reaches a new value, and the sol continues to exhibit the dampened band for extended periods of time (a few weeks) if left undisturbed. Several bivalent metal ions were examined. It was found that different metal ions cause the dampening of the plasmon band to different extents. For example, 80 μM Cu^{2+} solution brings about an ∼60% dampening of the plasmon intensity, but, on the other hand, 230 μM Fe^{2+} brings about a decrease of ∼50% (Figure 2). It is known that a change in the ionic strength causes aggregation of the sols, thus bringing about such changes in the plasmon band intensity. In the example above, the change in the ionic strength is around three times greater in case of Fe^{2+} ions than in the case of Cu^{2+} ions, but this change is not reflected in the dampening of the plasmon band. We therefore consider the observed dampening of the plasmon band to arise from a process that is selective to a particular metal ion, which involves the surface carboxyl group, rather than from the ionic strength of the medium. Accordingly, the sensitivity of the plasmon band varies from one metal ion to another.

To ascertain that this is indeed the case, we sought to remove the chelated metal ions by employing a ligand stronger than α-lipoic acid. Accordingly, by the addition of equimolar amounts of EDTA to Au and Ag sols containing chelated metal ions, it was possible to enhance the plasmon-band intensity to a value obtained in the absence of metal ions.

TEM studies shed further light on the above-mentioned change undergone by the colloid. In Figure 3, we show typical
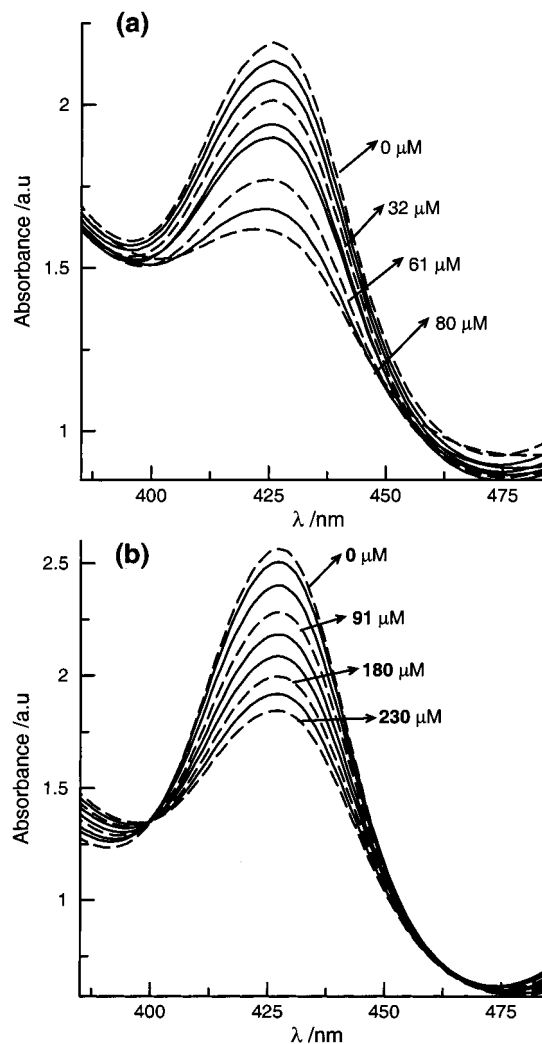
Figure 2. Electronic absorption spectra of ∼5-nm Ag nanoparticles showing changes accompanying the addition of (a) Cu^{2+} and (b) Fe^{2+}. The concentrations of the ions are indicated.

TEM micrographs of the ∼5-nm Ag nanoparticles before and after the addition of Cu^{2+} (80 μM) ions. We see that even in the presence of Cu^{2+} ions the nanoparticles remain isolated, with the aggregation[13] limited to very small areas (about 3% of

Effects of Chelation on Ag and Au Nanoparticles

J. Phys. Chem. B, Vol. 106, No. 18, 2002 **4649**
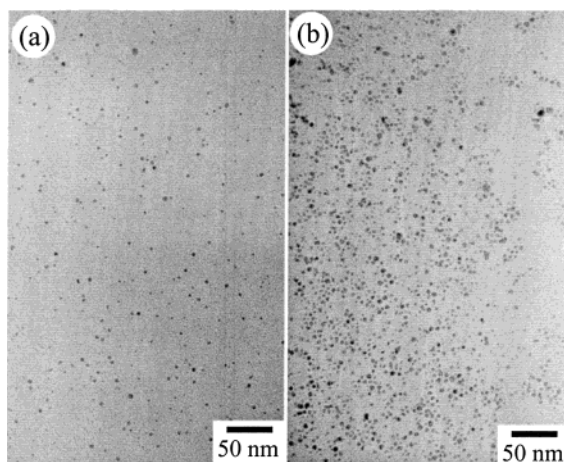
Figure 3. Electron micrographs of ∼5-nm Ag nanoparticles (a) before the addition of Cu^{2+} and (b) in the presence of 80 μM Cu^{2+}.
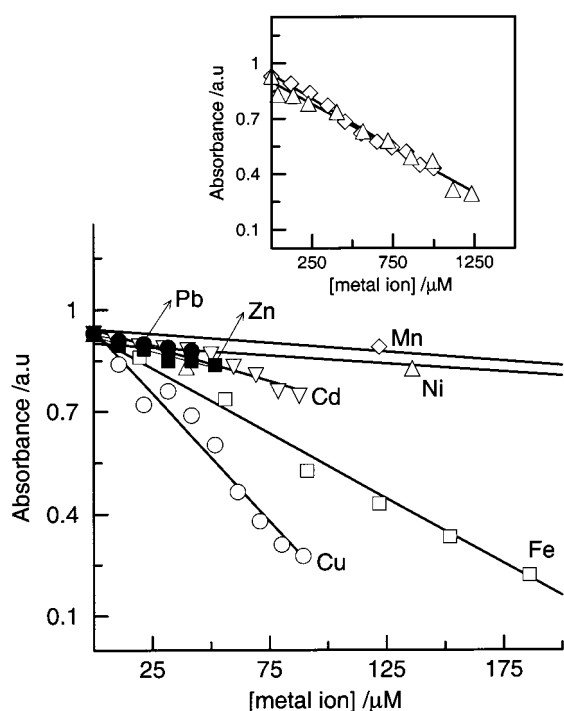
Figure 4. Variation in the absorbance of the plasmon band (at λ_{max}) of ∼5-nm Ag nanoparticles as a function of the concentration of metal ions. Linear fits are shown. The inset shows the data for Mn^{2+} and Ni^{2+} over an extended concentration range.

Figure 5. (a) Electronic absorption spectra of ∼7.5-nm Au nanoparticles showing changes accompanying the addition of Cu^{2+}. (b) Plots showing the variation of absorbance of the plasmon band (at λ_{max}) of Au nanoparticles accompanying the addition of Cu^{2+} ions. The circles correspond to nanoparticles of ∼7.5-nm diameter, and the squares correspond to ∼3.0 nm diameter nanoparticles.

the scanned area). This observation rules out aggregation as the cause of the observed dampening of the plasmon band. Theoretical investigations suggest that aggregates measuring a few hundred to a few thousand nanoparticles are required to obtain a substantive optical response.[14] The binding of metal ions appears to proceed more by path a than by path b in Figure 1.

Dampening of the plasmon band (along with accompanying changes in position and width) arising from the chemisorption of reactive molecules on the surfaces of nanoparticles[2,5,15] had earlier been attributed to charge transfer between the particle and the adsorbate. We have not found any change in the position or the width of the plasmon band accompanying the chelation of metal ions, but instead we observe only a decrease in the band intensity. The existence of an isobestic point at 399 nm in Figure 2b and the nearly constant absorbance at 460 nm corroborate this view. Even where there is no isobestic point

as in Figure 2a, there is little shift in the position of the width of the plasmon band. The trends were similar with different counteranions. Similar changes in the plasmon-band intensity were observed for Ag nanoparticles with a mean diameter of 2.6 nm following chelation. It can therefore be concluded that in the dilute metal-ion concentration regime the metal ions bind to the carboxyl functional group of α-lipoic acid, which caps the nanoparticles and thereby causes the observed dampening of the plasmon band.

The ability of metal ions to dampen the plasmon band has been quantified by making use of the slopes of the plots of the plasmon-band intensity against the metal-ion concentration. We present such plots of the absorbance of the plasmon band of Ag nanoparticles at the absorption maximum against the concentration of metal ions. We also show the corresponding linear fits in this Figure. The inset in Figure 4 shows that the intensity decrease can continue over an extended region of concentration in the case of weakly interacting metal ions such as Mn^{2+} and Ni^{2+}. The values of the slopes ($\times 10^3$ M^{-1}) for the interactions of Cu^{2+}, Fe^{2+}, Cd^{2+}, Zn^{2+}, Pb^{2+}, Mn^{2+}, and Ni^{2+} with ∼5-nm Ag nanoparticles are 7.5, 3.8, 2.0, 1.8, 1.2, 0.5, and 0.5 ×, respectively. The slopes ($\times 10^3$ M^{-1}) obtained for Ag nanoparticles with a mean diameter of 2.6 nm were 2.8,
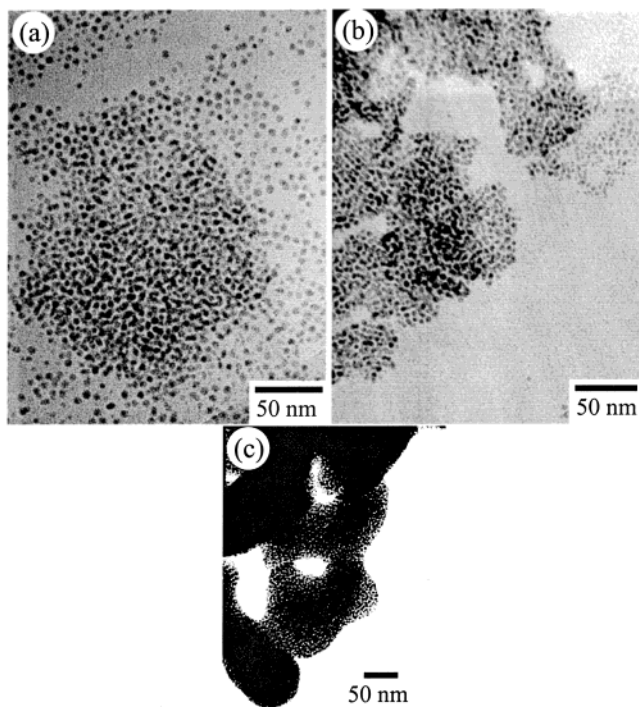
Figure 6. Electron micrographs of ∼5-nm Ag nanoparticles after interaction with aqueous Cu^{2+} solutions that are (a) 120 μM, (b) 200 μM, and (c) 500 μM.

0.6, 0.5, and 0.2 ×for Cu^{2+}, Fe^{2+}, Mn^{2+}, and Ni^{2+} ions, respectively. Similar results were obtained when the counterions of the Cu, Ni, and Mn ions were changed to chlorides. Although the slopes of the absorption−concentration plots are higher when the particle diameter is larger, the effectiveness of chelation varies in the order Cu^{2+} > Fe^{2+} > Mn^{2+} > Ni^{2+} and is independent of the diameter of the Ag nanoparticles.

Figure 5 shows the results of our studies on the interaction of Cu^{2+} ions with Au nanoparticles. In Figure 5a, we present the changes in the absorption spectra of the ∼7.5-nm Au nanoparticles brought about by the addition of Cu^{2+} ions. A decrease in the plasmon-band intensity is observed just as in the case of Ag nanoparticles. In Figure 5b, we show the change in the absorbance with the Cu^{2+} concentration for 7.5- and 3.0-nm Au nanoparticles. The slope is slightly greater in the case of the larger Au nanoparticles.

Addition of Cu^{2+} ions to ∼5-nm Ag nanoparticles beyond the dilute regime (>90 μM) brings about different changes in the sol. The sols precipitate after about 200 μM Cu^{2+} has been added. The onset of precipitation is shifted to higher concentration upon addition of PVA(5%). TEM studies indicate that the nanoparticles form aggregates, with the extent of aggregation (measured as the fraction of particles belonging to an aggregate) increasing with the concentration of the metal ions, as shown by the micrographs in Figure 6. When the Cu^{2+} concentration is 120 μM (Figure 6a), ∼50% of the nanoparticles form aggregates, which is in contrast to the case of 80 μM Cu^{2+} where the aggregation is limited to ∼3% of the particles (see Figure 3b). Almost all the particles get aggregated when the concentration of Cu^{2+} is raised to 200 μM. We note that the sols showed little sign of opalescence and remained stable during all of the measurements discussed hitherto (in the Cu^{2+} concentration regime of 0−200 μM). Further addition of Cu^{2+} ions, however, leads to precipitation. TEM images of the precipitate showed multilayered, close-packed structures of nanoparticles (Figure 6c).
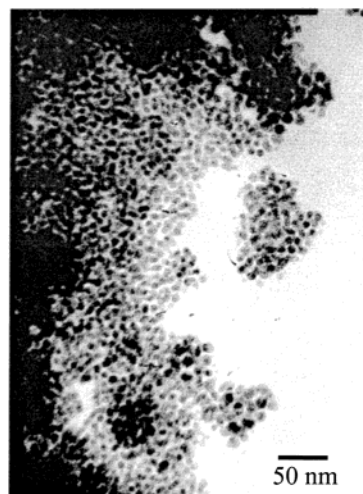
Figure 7. Electron micrographs of ∼7.5-nm Au nanoparticles after interaction with an aqueous 600 μM Cu^{2+} solution.
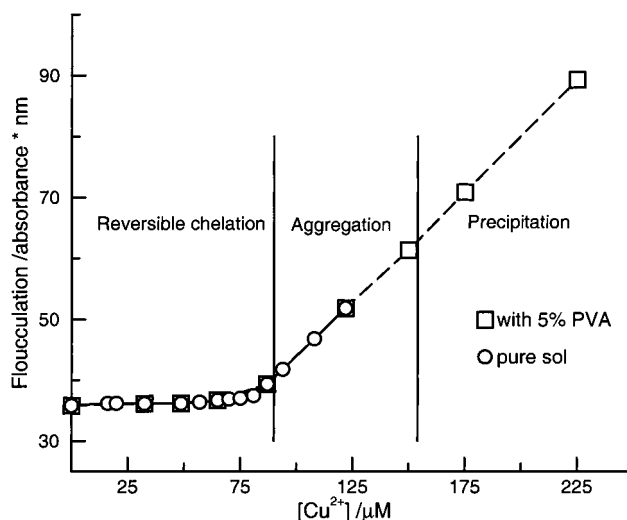
Figure 8. Variation of the floucculation parameter with the concentration of Cu^{2+} in the case of 5-nm Ag nanoparticles.

The above observations are supported by changes in the optical spectra of the nanoparticles. In the above concentration regime (90 μM < [Cu^{2+}] > 200 μM), the plasmon band is completely damped, and the scatter at longer wavelengths, which was essentially constant in the dilute regime, increases progressively. To quantify the changes, we employ a slightly modified version of the floucculation parameter defined previously by Weisbecker et al.[6] for Au colloids. The floucculation parameter, defined here for the case of Ag nanoparticles as the integrated area in the 550−750 nm region, shows an increase with the metal ion concentration that coincides with aggregation phenomena described previously. The change in the floucculation parameter could not be reversed by addition of EDTA, and thus the chelation is *irreversible*. Addition of PVA stabilizes the sol and permits further addition of Cu ions with higher values of the floucculation parameter than that of the native sol. We thus have a regime of chelation that is not reversible by addition of stronger chelating agents above 90 μM Cu^{2+}, followed by a regime where precipitation occurs (Figure 6c). In the case of Au nanoparticles, the region of irreversible chelation was also marked by aggregation, as can be seen from the TEM micrograph in Figure 7.

The different regimes of metal-ion interaction with α-lipoic acid-capped Ag nanoparticles, delineated on the basis of the floucculation parameter, are depicted in Figure 8. In the case

Effects of Chelation on Ag and Au Nanoparticles

J. Phys. Chem. B, Vol. 106, No. 18, 2002 **4651**

of other metal ions such as Fe^{2+} and Cd^{2+}, the different regimes occur at concentrations different from those found with Cu^{2+}, as expected on the basis of the slopes in the absorbance−concentration plots (Figure 4).

The observation that the aggregates and the precipitates are made of nanoparticles similar in dimensions to those of the colloid and the fact that the onset of aggregation depends on the metal ion used seem to suggest that the binding event (chelation) is responsible for aggregation and precipitation. However, given that the aggregation and precipitation are irreversible and that the stabilizing agent PVA is able to shift the onset of precipitation, we find that the ionic strength of the medium may indeed play a role. The actual factors leading to aggregation and precipitation, in the case of α-lipoic acid-capped Au and Ag nanoparticles, may well involve a combination of both of these factors.

Conclusions

The present study shows three distinct regimes of interactions of metal ions with α-lipoic acid-capped Ag nanoparticles, the regime of low metal-ion concentration being associated with reversible chelation and dampening of the plasmon band. Aggregation and irreversible chelation accompanied by an increase in the flocculation parameter characterize the regime of intermediate metal-ion concentration. Further increases in metal-ion concentration result in precipitation.

References and Notes

(1) Link, S.; El-Sayed, M. A. *J. Phys. Chem. B* **2001**, *105*, 1; Link, S.; El-Sayed, M. A. *Int. Rev. Phys. Chem.* **2001**, *19*, 409.

(2) Mulvaney, P. *Langmuir* **1996**, *788*, 12.

(3) Seshadri, R.; Subbanna, G. N.; Vijayakrishnan, V.; Kulkarni, G. U.; Ananthakrishna, G.; Rao, C. N. R. *J. Phys. Chem. B* **1995**, *99*, 5639.

(4) Mirkin, C. A.; Letsinger, R. L.; Mucic, R. C.; Storhoff, J. J. *Nature (London)* **1996**, *382*, 607.

(5) Linnert, T.; Mulvaney, P.; Henglein, A. *J. Phys. Chem. B* **1993**, *97*, 679.

(6) Weisbecker, C. S.; Merritt, M. V.; Whitesides, G. M. *Langmuir* **1996**, *12*, 3763.

(7) Mayya, K. S.; Patil, V.; Sastry, M. *Langmuir* **1996**, *13*, 3944.

(8) Schmitt, H.; Badia, A.; Dickson, L.; Reven, L.; Lennox, R. B. *Adv. Mater. (Weinheim, Ger.)* **1998**, *10*, 475.

(9) Templeton, C.; Zamborini, F. P.; Wuelfing, W. P.; Murray, R. W. *Langmuir* **2000**, *16*, 6682.

(10) Kim, Y.; Johnson, R. C.; Hupp, J. T. *Nano Lett.* **2001**, *1*, 165.

(11) Simard, J.; Briggs, C.; Boal, A. K.; Rotello, V. M. *Chem. Commun.* **2000**, 1943.

(12) Maya, L.; Muralidharan, G.; Thundat, T. G.; Kenik, E. A. *Langmuir* **2000**, *16*, 9151.

(13) Throughout this paper, we make no distinction between aggregation, which is the close, irreversible association of primary particles, and agglomeration, which is loose, reversible association. The floucculation parameter used here takes into account the contribution from both aggregates and agglomerates and follows the definition of Weisbecker et al.[6]

(14) Lazarides, A. A.; Schatz, G. C. *J. Phys. Chem. B* **2000**, *104*, 460; Lazarides, A. A.; Schatz, G. C. *J. Chem. Phys.* **2000**, *112*, 2987.

(15) Strelow, F.; Henglein, A. *J. Phys. Chem. B* **1995**, *99*, 11834; Strelow, F.; Fojtik, A.; Henglein, A. *J. Phys. Chem. B* **1994**, *98*, 3032; Henglein, A.; Meisel, D. *J. Phys. Chem. B* **1998**, *102*, 8364.